

Investigation of the Mechanical Behavior of Full-Scale Experimental Bugis-Makassar Timber House Structures

Armin Aryadi^{1, 2*} , Herman Parung¹, Rita Irmawaty¹ , Andi A. Amiruddin¹ 

¹ Department of Civil Engineering, Faculty of Engineering, Hasanuddin University, Gowa, Indonesia.

² Department of Civil Engineering, University of 19 November Kolaka, Kolaka 93514, Indonesia.

Received 03 February 2024; Revised 02 May 2024; Accepted 09 May 2024; Published 01 June 2024

Abstract

The Sulawesi region is located at the confluence of a smaller Philippine plate and three major global plates, namely the Indo-Australian, Pacific, and Eurasian. This strategic location makes Sulawesi and the surrounding earthquake-prone region in Indonesia. Recognizing the seismic vulnerability of this region, various measures, such as the use of houses on stilts, have been explored to enhance earthquake resistance. These structures are designed to avoid direct exposure to seismic energy, according to several reports on Indonesian earthquakes. In the last two years, an in-depth investigation has been carried out to analyze the behavior and resistance of Bugis Traditional Houses to earthquakes. Although simulation and computational studies are still in progress, the results show that Bugis-Makassar House on stilts maintains an elastic state with a high level of performance. Therefore, this study aimed to investigate the mechanical behavior of Bugis-Makassar stilt house structures using full-scale tests. During the investigation, experimental testing was conducted using house specimens measuring 1.5×2.3 m in the laboratory. A cyclic lateral loading analysis was performed using ISO 16670-2003 as a guide. The results showed that cyclic lateral loads caused house structures to sway, while the timber experienced minimal damage. Both the hysteresis energy, E_H to E_I , and the energy conversion ratio, GPE to ESE (E_R), were found to be approximately balanced. This equilibrium suggested that seismic energy can be cyclically stored and released to reduce damage to structural elements.

Keywords: Earthquake; Timber House Structure; GPE and ESE Energy (E_R); Hysterical Energy; Input Energy.

1. Introduction

Indonesia is an archipelagic region with a unique geographical setting at a triple junction, where three actively moving tectonic plates converge in the form of faults and the most active volcanoes in the world [1]. The Pacific Plate moving relatively westward at a rate of 12 cm per year influences the geology of Sulawesi Island, resulting in complexity due to the intrusion of the Indo-Australian Plate into the relatively stationary Eurasian Plate at 7 cm per year in the north. This interaction creates various plate movements, including subduction pathways that actively contribute to earthquake activity as well as the development of local and regional faults. Over the past 20 years, Indonesia has garnered international attention due to catastrophic natural disasters that have destroyed the nation's infrastructure and claimed hundreds of thousands of lives [2]. Because Indonesia is located in the Ring of Fire, earthquakes frequently occur there [3]. The arc of Indonesia is part of the Pacific Ocean's Ring of Fire, where multiple tectonic plates are crashing together. On September 28, 2018, a powerful earthquake—one of the strongest since 1980—struck Palu, Sulawesi Island, Indonesia [4]. Widespread destruction was brought about by the 1.5 m tsunami waves that struck Palu and Donggala and the 7.5-magnitude earthquake that struck Central Sulawesi. Authorities in Indonesia estimate that the disaster

* Corresponding author: civilarchitects.aryasi@gmail.com, arwin_amiruddin@unhas.ac.id

 <http://dx.doi.org/10.28991/CEJ-2024-010-06-04>



© 2024 by the authors. Licensee C.E.J, Tehran, Iran. This article is an open access article distributed under the terms and conditions of the Creative Commons Attribution (CC-BY) license (<http://creativecommons.org/licenses/by/4.0/>).

affected 2.4 million people. Surprisingly, the majority of Sulawesi's traditional homes survived this catastrophe [5, 6]. The Indonesian traditional house was shaped by its surroundings, which were reflected in peoples' daily lives and served as a symbol of their culture [7]. This strategic location makes Sulawesi Island and the surrounding earthquake-prone region in Indonesia.

The seismic vulnerability was evident in the earthquake that struck Mamuju City on January 15, 2021. According to BMKG, this earthquake had an intensity of VI MMI, with peak vibrations measured at 150 gal (1.5 m/sec²), causing several buildings to collapse due to the damage. As shown in Figure 1-a, when an earthquake struck, the Mamuju Traditional House was still intact, sustaining only minor damage to the walls and other structural components. East Nusa Tenggara (NTT) also experienced an earthquake with a magnitude of 7.5 on December 14, 2021, due to a strike-slip fault system that reached South Sulawesi [8]. In this case, the NTT earthquake, as shown in Figure 1-b, caused the walls of a resident house to collapse, showing a neighboring wooden stilt house that was still standing. This comparison shows the crucial role of proper building design in preventing or minimizing fatalities during seismic events, emphasizing resilient structures [9].

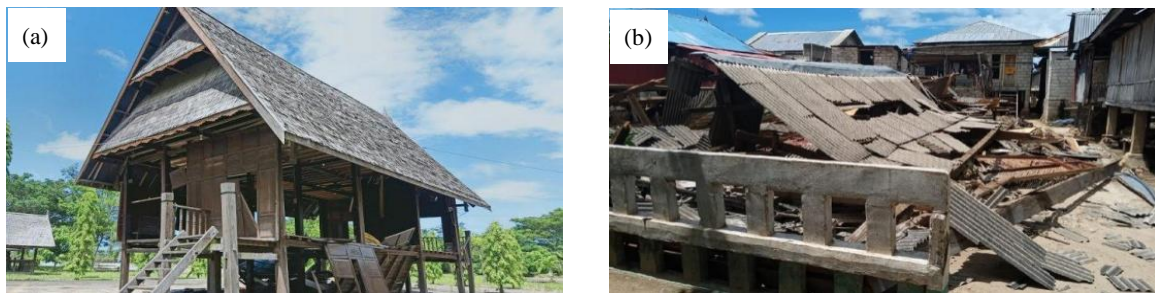


Figure 1. a. Mamuju traditional house (Mamuju Earthquake) b. House of Walls and Selayar Island Residents' Wooden Stilt Houses (NTT Earthquake)

Bugis-Makassar Stage Houses, along with the traditional form of Mamuju share several similarities, differing only in terminology due to dialect and language variations. Moreover, Bugis-Makassar houses are characterized by stilt-like shapes, gable roofs, and *timpalajas* with a specific number of arrangements, serving as a symbol of the owner's social standing. In terms of structure, the Bugis-Makassar houses are divided into three sections, namely the top portion or roof, middle, and bottom or pillar, which are comparable to the human body, representing head, body, and foot, respectively.

Figure 2 shows the composition of the main structure, comprising multiple independently constructed (knock-down) parts. The cultural traditions of South Sulawesi have demonstrated efficacy in mitigating seismic activity in the past and may be able to withstand future seismic events in the area. When it comes to mitigating the effects of earthquakes in residential buildings, local knowledge is invaluable. It was discovered that the corridor (*tamping*) in Bugis-Makassar houses is the best place to evacuate [10].

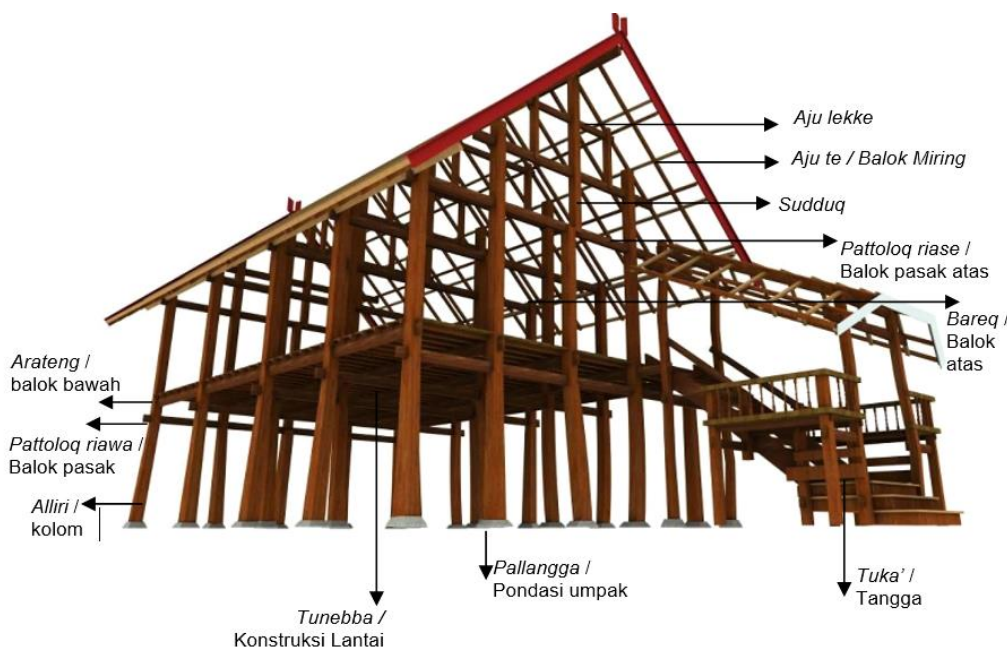


Figure 2. Structural Perspective of Bugis-Makassar Stilt Houses

However, the demand for quick and simple buildings has increased recently due to global events such as pandemics, migrant flows, resource depletion, increasing poverty, war, and natural disasters. These events have led to a need for modular and flexible knock-down houses that can be repurposed without sacrificing comfort or environmental sustainability [11].

Houses on stilts are considered earthquake-resistant due to the ability to avoid direct exposure to seismic energy. According to Doğan (2005) [12] and Doğangün (2010) [13], it was established that traditional Turkish houses are more earthquake-resistant compared to contemporary constructions. However, wooden buildings and wood-frame construction have proven to be exceptionally resilient during earthquakes in various regions globally, including Turkey [14–17], the Indian Himalayan [18, 19], Nepal [20], Kaikoura, New Zealand [21], Japan [22], and Korea [23]. Traditional wood frame construction has shown better resistance to past earthquake events compared to unreinforced masonry walls [24]. Furthermore, traditional Chinese wood frame structures with wood panels (infill walls) show higher results regarding load capacity, stiffness, and better energy dissipation compared to frames without wood panels [25].

In light of current global occurrences pertaining to sustainability and environmental concerns, wood-framed structures are potentially carbon-absorbing structures of the future. According to research by Dzhurko et al. (2024), there is a significant reduction in carbon emissions during the building production stage when traditional mineral-based building materials are replaced with biomass-based materials like wood. It seems that newly constructed buildings composed of typological wood have a high potential for storing carbon within the building's main structure, which can increase the carbon sink capacity of surrounding neighborhoods or cities as a whole [26]. The research on novel structural systems for wooden buildings adds to our understanding of modern solid wood and hybrid wood structural system solutions and how they are used in multi-story wooden buildings. This is a novel development in the field of wood construction review [27].

An experimental analysis of the structural performance of traditional pre-Ming dynasty building construction at a scale of 1: 2 under cyclic lateral loads was carried out Meng et al. (2018) [28]. During testing, wooden structure showed observable swaying, with the column legs and mortise-tenon joints identified as the weakest points. The results indicated essential characteristics of wooden structures, including envelope curve, hysteresis curve, strength loss, energy dissipation, and lateral stiffness, with varied cyclic lateral loading programs. A comprehensive experimental study has also been conducted on the seismic performance of South Chinese traditional Chuan-Dou model wooden frames [29].

The results showed that the Chuan-Dou model wooden frame performed regarding energy dissipation, strength degradation, and capacity deformation. However, the presence of insufficient lateral stiffness showed the need to address the critical role of joints in frame performance. Meng et al. (2019) conducted a full-scale experimental study on seismic performance, considering the vertical lifting of structures during lateral loading [30]. The results showed how large-scale earthquake resistance is provided by the energy conversion to gravitational potential energy (GPE) mechanism in traditional Chinese wooden structures. Similarly, Sha et al. (2021) investigated the hysteretic behavior of Ancient Chinese multi-layer wooden structure construction through a full-scale substructure model comprising mortise-tenon joint frames and fork-column dou-gong joints that were tested under cyclic load [31]. The results showed that the dou-gong layer's stiffness was 6.5 to 14.3 times greater than frame layer, absorbing a greater portion of the load displacement.

In their experimental study on the inelastic behavior of mortise-tenon (SMT) joints in traditional wood frames with freestanding columns (CF), Yu et al. (2023) found that plastic deformation of wood frames primarily occurs at SMT joints perpendicular to the grain, with parallel plastic deformation having an impact on CF. Wooden frames exhibit trilinear properties in their lateral resistance, which makes them comparatively low [32]. The mutual friction between the mortise and tenon has a certain energy dissipation and shock absorption effect, according to additional experimental research by Ren et al. (2024) [33] on an experimental study on the strengthening of wooden pins in typical mortise-tenon joints in ancient wooden frames. Additionally, the strengthening of wooden pins effectively controls the horizontal displacement of the frame wood, which is reduced by approximately 50%–62% compared to unreinforced wood frames. Additional experimental research on the seismic performance of through-tenon wood joints with shrinkage weaknesses in the tenons was carried out by Li et al. (2023) [34]. The results show that experimental curves of hysteresis, frame, energy dissipation, and stiffness were obtained; in addition, the damaged joints' rotational capacity, stiffness, and energy dissipation capacity were significantly lower than those of the intact joints [34].

Previous studies in the last two years on Bugis-Makassar Traditional Houses have focused on architectural form and space [35, 36], along with cultural society [37] investigating the behavior and earthquake resistance of the structures. Despite being in the simulation and computational stages, Puspitasari et al. (2022) [38] expressed concerns about insufficient structural strength. According to additional simulation studies, the performance and response analysis of Bugis-Makassar Stage Houses are still at a high level and in an elastic state [39]. Therefore, this study aimed to conduct a full-scale mechanical behavior analysis of Bugis-Makassar stilt house structures.

There are structural and design differences between Bugis-Makassar wooden stilt houses and traditional wooden houses in China that affect how well they can withstand earthquake loads. Traditional Chinese wooden homes have stronger, stiffer structural components that can withstand the vibrations caused by earthquakes. The thick wooden walls

and curved tiled roof give the structure extra strength against the lateral forces produced by earthquakes. The stilt structure of traditional Bugis-Makassar stilt houses elevates the house above the ground, which may be advantageous in attenuating seismic vibrations that are absorbed by the earth. However, flat or sloping roof designs made of zinc or palm fiber might not offer the same level of defense against the lateral forces produced by earthquakes. Chinese wooden houses typically consist of hardwood materials like pine and cypress, which are more resilient to lateral pressure brought on by earthquakes. The majority of the wood used to build Bugis-Makassar stilt houses comes from the surrounding area. Woods like teak, ironwood, meranti, and bitti are more flexible than hardwood and are better at absorbing earthquake vibrations. But the wood's strength and quality must also be taken into account.

An approach that combines the best features of both traditions while preserving their distinctive qualities may be necessary to bridge the structural gap between Bugis-Makassar wooden stilt houses and traditional wooden houses in China when it comes to withstanding earthquake loads. The best course of action is to conduct additional research to determine which wood species and building materials combine the best qualities of strength, elasticity, and earthquake resistance; to adopt structural design elements that have worked well in both traditions for example, utilizing the more durable support system of Chinese wooden houses while preserving the structural flexibility of Bugis-Makassar stilt houses and to conduct tests and earthquake simulations on engineered house models to make sure that the house's structure and design can withstand seismic activity. Combining these strategies can help close the structural gap that exists between Bugis-Makassar wooden stilt houses and traditional wooden houses in China in terms of how each cultural tradition responds to seismic loads while preserving its individuality and authenticity. This serves as the context in which the author will carry out additional experimental research. The purpose of this study is to conduct a full-scale mechanical behavior analysis of Bugis-Makassar stilt house structures.

2. Materials and Method

2.1. Materials

The material objects for the stilt house structure in this study are obtained from Bulukumba Regency's eastern area. As shown in Figure 3, all structural elements, including pillars, tie beams, roof construction, floor, and ceiling support frames, are made of native Bitti wood. Natural habitats for bitti wood include Sulawesi, Maluku, Papua New Guinea, the Bismarck Islands, and the Solomon Islands. In addition to being fire resistant, bitti wood can regenerate after burning, suggesting the potential evolution into a more advanced species [40].

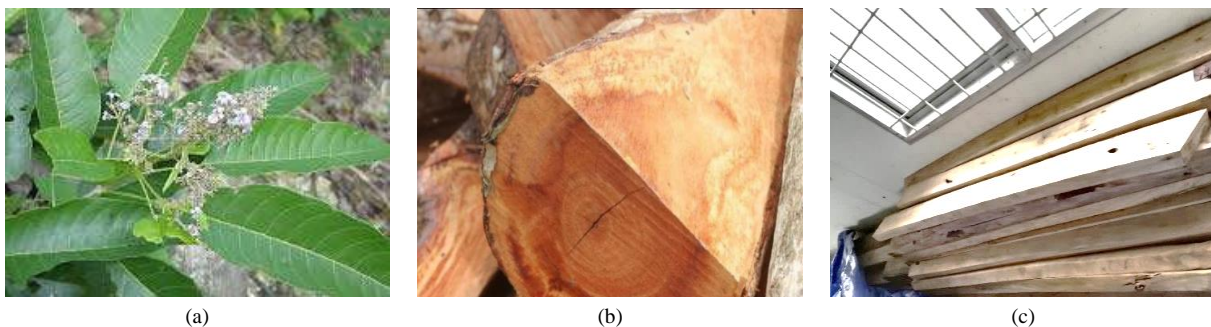


Figure 3. (a) Bitti wood leaves and flowers, (b) Bitti wood stems, (c) Bitti wood structural components

Burley et al. (2011) stated that Bitti wood (*Vitex cofassus*), Angsana (*Pterocarpus indicacus*), and Walnut (*Canarium indicum*) are classified as early successional trees [41]. Moreover, Bitti Wood Reference Strength for Fb 10.07 MPa, Ft 8.90 MPa, Fc// 8.90 MPa, Fv 1.18, and Fc⊥ 2.37 MPa is derived from visual sorting. This information is included in the E 11 wood quality based on SNI 7973: 2013, where $E_w = 11566.271$ Mpa and $E_{min} = 5405.821$ Mpa. Specifically, Bitti Wood Reference Strength for Fb 95.40 MPa, Ft// 54.90 MPa, Ft⊥ 3.10 MPa, Fc// /40.2 MPa, and Fc⊥ 88.30 MPa is derived from mechanical sorting [42].

2.2. Research Methodology

The flow of research conducted in this study is presented in Figure 4. Bitti wood, commonly used in Bugis-Makassar stilt houses, serves as the foundation for constructing a full-scale wooden model. The design includes shape and structural dimensions, obtained from the structural model and Bugis-Makassar stilt houses as standard prototype test specimens [43]. The model comprises columns (*alliri*), bottom beam, top beam, bottom post beam, top post beam, and floor beam, as illustrated in Figures 5. The concrete floor is directly beneath the columns, mimicking the connections between free supports found in actual wooden buildings. Subsequently, columns are joined to beams and post beams using mortise-tenon connections and post-reinforcement. *Aju lekke*, *Aju te*, and *sudduq* serve as the parts constituting the roof frame structure, with *sudduq* having a pin support on the upper peg beam as a column. Table 1 lists the dimensions of wooden components, while Figure 5 shows details of the beam-column connection with peg reinforcement and *sudduq* with clamp supports on the top beam.

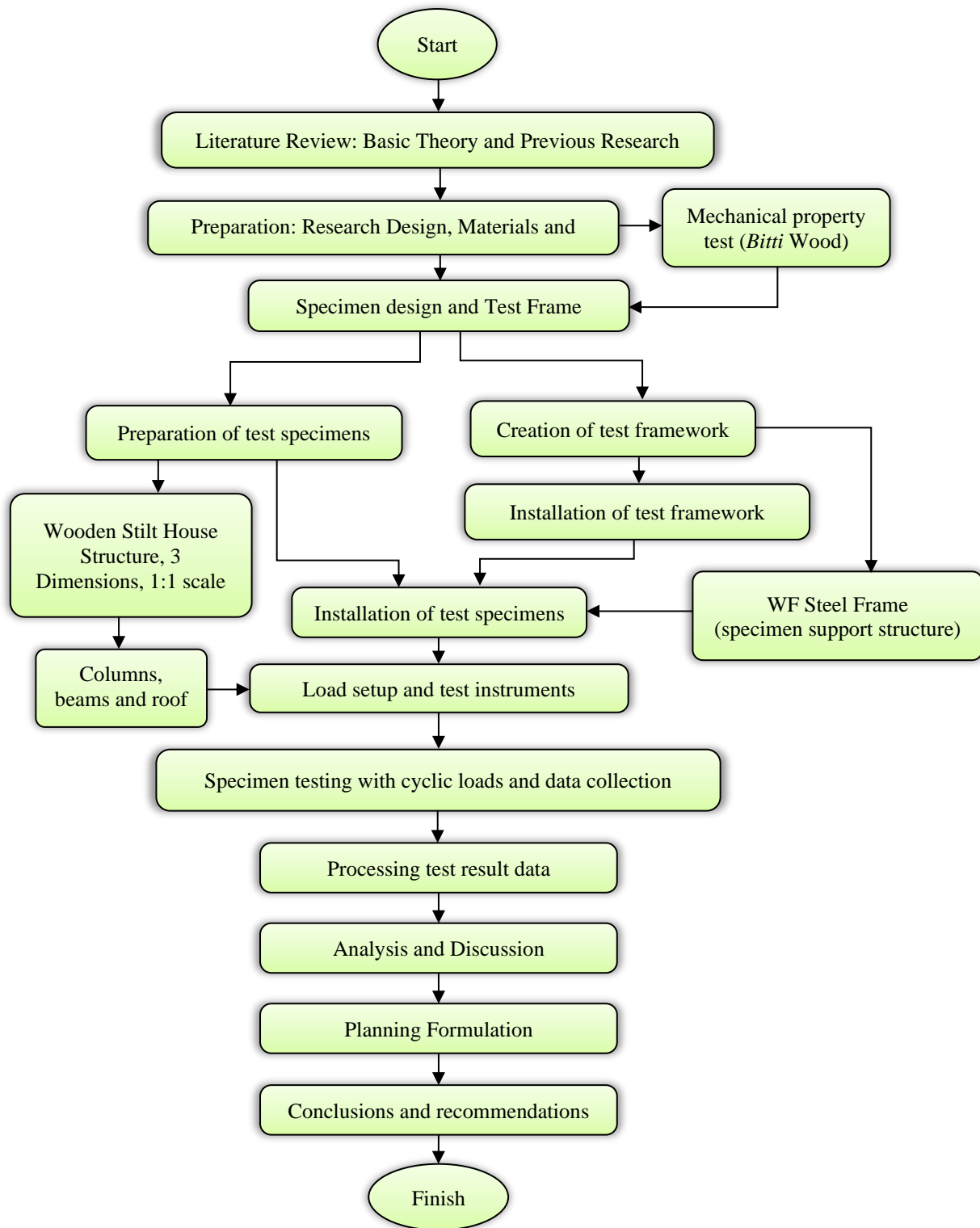
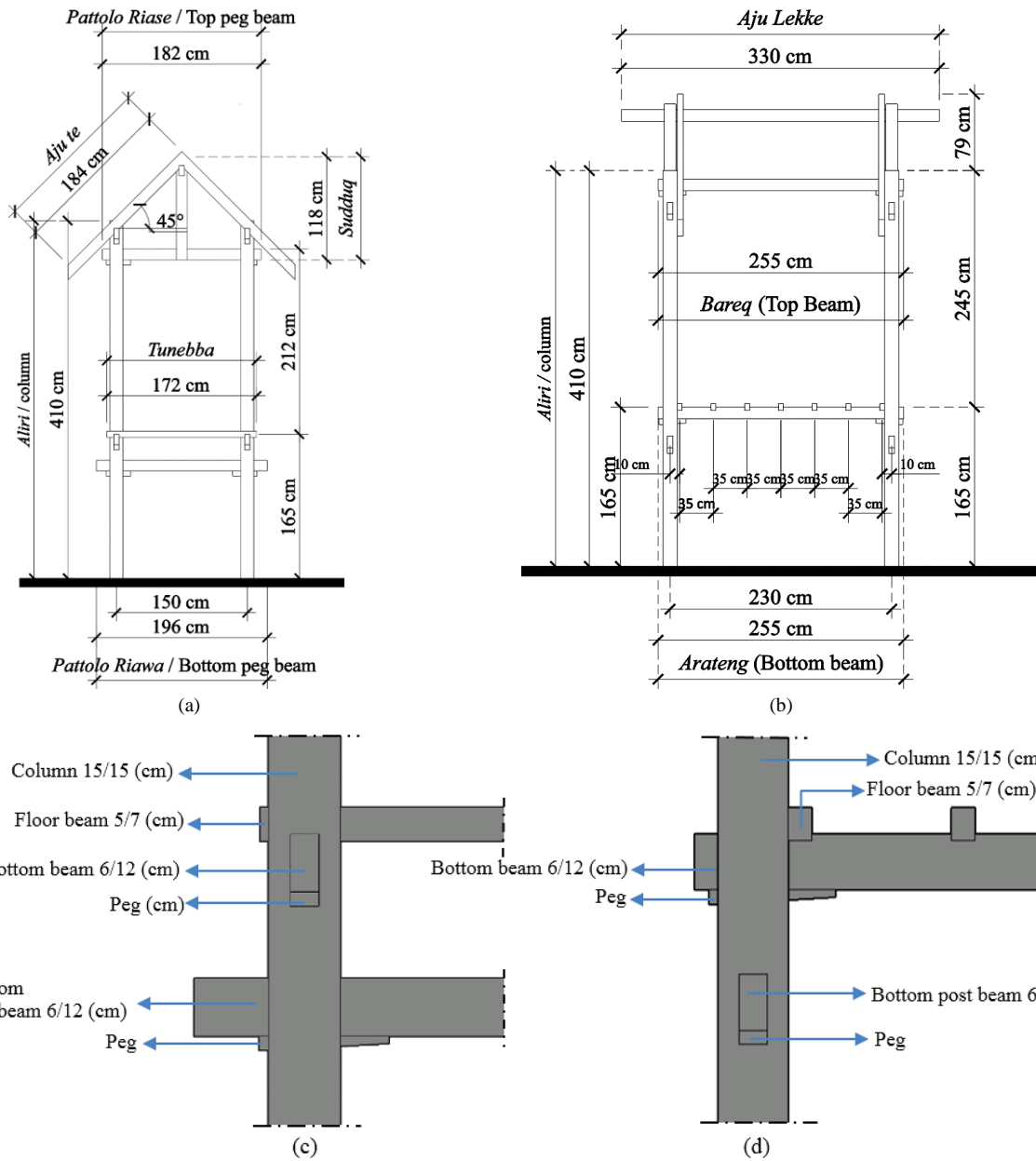


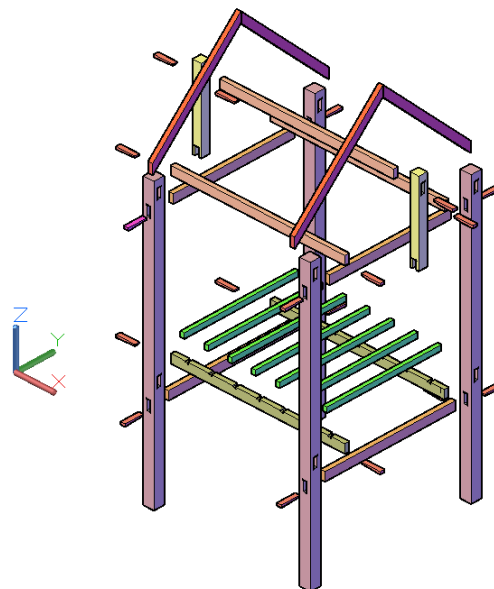
Figure 4. Research methodology flowchart

Table 1. Size of Stilt House Structural Components

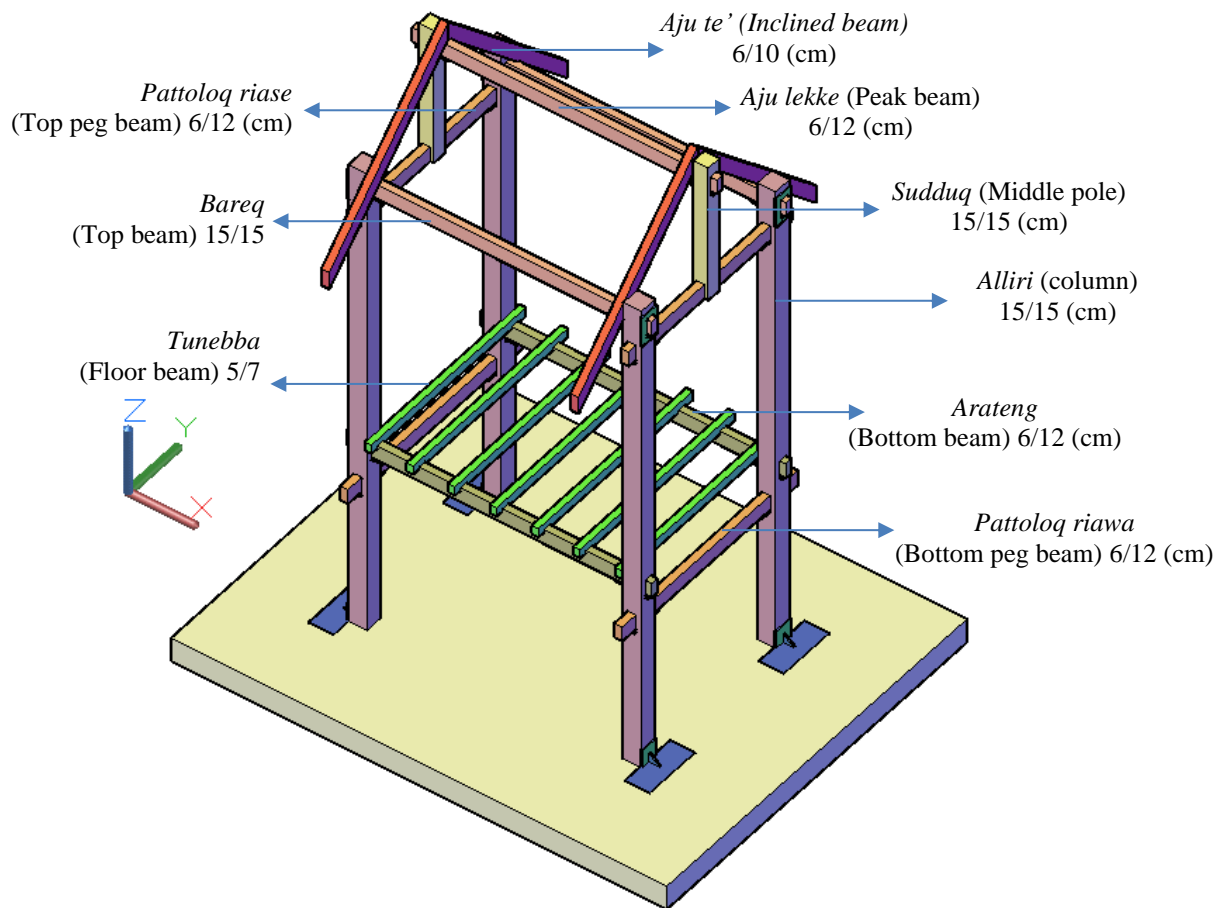
Component	Wood Size (cm)	Extended (cm)	Component	Wood Size (cm)	Extended (cm)
<i>Alliri</i> (Column)	15×15	410	<i>Sudduq</i> (Middle pole)	15×15	118
<i>Arateng</i> (Bottom beam)	6×12	255	<i>Aju lekke</i> (Peak beam)	6×12	330
<i>Bareq</i> (Top beam)	6×12	255	<i>Aju te'</i> (Inclined beam)	6×10	184
<i>Pattoloq riawa</i> (Bottom peg beam)	6×12	196	<i>Tunebba</i> (Floor beam)	5×7	172
<i>Pattoloq riase</i> (Top peg beam)	6×12	182	<i>Pa'pasa</i> (Peg)		



(i). Design of Specimen Models: a) Frontal view, b) Side view; c) detail 1 - column-beam connection, d) detail 2 - column-beam connection



(ii). Assembly of Structural Components the Bugis-Makassar Stage House



(iii). 3D Specimen Model the Bugis-Makassar Stage House

Figure 5. Details of the structure

As part of the test preparations, test site specimens of house structural elements, such as columns, beams, and roof frames, were assembled. The assembled specimen is subsequently placed atop the initially installed support structure. Following that, the horizontal jack (actuator) installation is carried out. In order to prevent excessive horizontal twisting of the specimen, a horizontal stiffening rod is installed at the top of the specimen. The specimen and test frame can be seen in Figure 6.

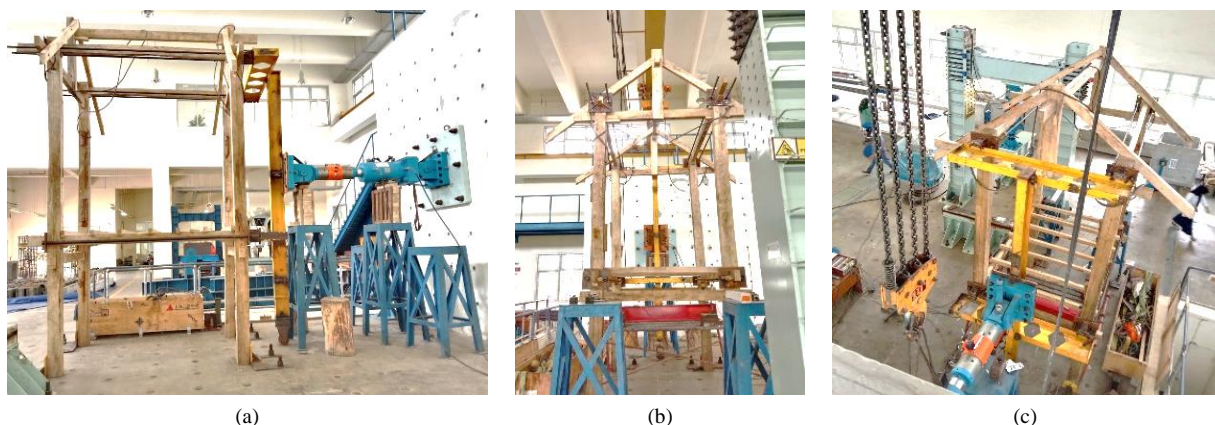


Figure 6. Full-scale specimen test model (a) Side view, (b) Frontal view, (c) Top view

2.2.1. Installing Testing Apparatus and Instruments, and Cyclic Lateral Loads

In this study, cyclic lateral loads were applied using a displacement-controlled synchronous loading device with reference to ISO 16670-2003. Subsequently, specimens were subjected to lateral loads in pull-push directions until the yield limit was reached, followed by further loads to failure. Regarding ISO 16670-2003 [44], Figure 7 shows the load

test based on the type and service, using displacement-controlled method comprising phases of displacement cycles with progressively higher rates. The first displacement pattern consists of five single fully inverted cycles at displacements of 1.25%, 2.5%, 5%, 7.5%, and 10% of the maximum load specified in the standard. The second displacement pattern is composed of phases at displacements of 20%, 40%, 60%, 80%, 100%, and 120% of the maximum displacement Δm , each with three cycles of equal inverse amplitude. The horizontal deformation of 0.02H in the SNI earthquake building planning rules (SNI 1726-2019) serves as the basis for determining Δm in this study.

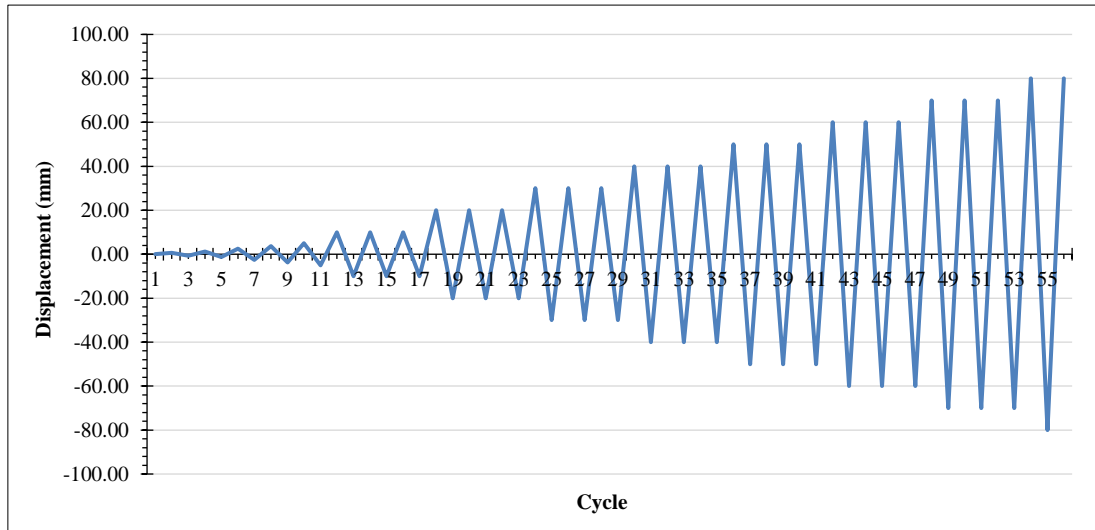


Figure 7. Loading type and load service, load test according to International Standards Organization (ISO 16670-2003)

Deflection and strain gauges are the two types of testing instruments used in this study and their locations are shown in Figure 8. The FLK 2.12 strain gauge is used for wood, positioned five centimeters from the column's edge at each intersection of the beam and column. A Linear Variable Displacement Transducer (LVDT) with an accuracy of 0.005, 0.01, and 0.02 was used as the deflection measuring device. To measure the horizontal deflection provided by an actuator, 1 (one) LVDT with an accuracy of 0.02 was mounted on the steel frame. Measurement of the horizontal deflection of the column elements was carried out using four LVDTs with an accuracy of 0.01 placed in the *Alliri* (column) area. The vertical deflection of the two beam elements in the *Arateng* area was measured using an LVDT with a 0.005 accuracy. Furthermore, the hydraulic jack (actuator) with a 1200 KN capacity and a maximum pushing and pulling distance of 20 cm each was used as the load-bearing apparatus. Additional equipment included a computer with a monitor, a data logger of type THS 1100, and a switching box of type SHW 500.



Figure 8. Placement of testing instruments (strain gauge) and LVDT

Installing the testing instruments and equipment networks as depicted in Figure 9. Data from every kind of instrument used is fed into the computer once all of the specimen's data cables have been connected to the switching box. The computer's data entry format is displayed in Figure 10.

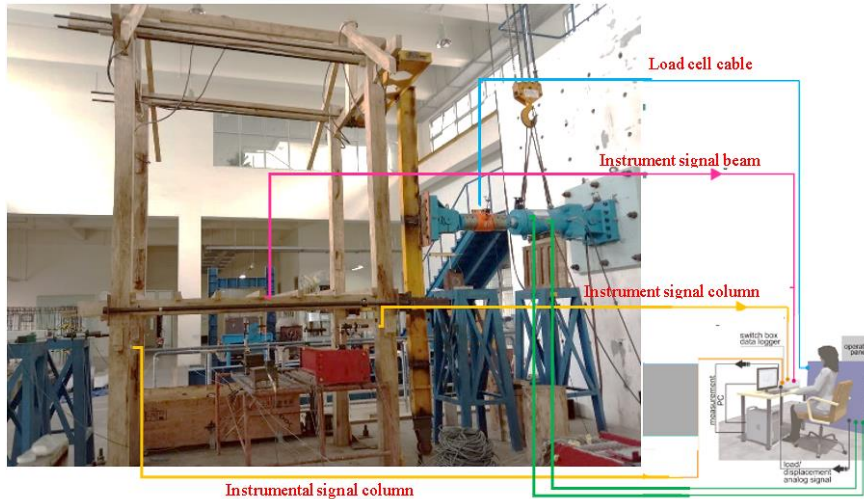


Figure 9. Equipment and instrument network installation (Instruction: Manual of Static Servo Controller System)

Visual LOG TDS-7130 - [CCB1-2.tsd]

File Edit Sheet View Measurement Window Help

Test Title: THS-1100 Step 5063

Condition setup		Interval setup	Data comparator setup	Data list	Data table	Check result	Option data			Alarm		
No.	Name	Ch.No./Function	Unit	Format	Meas/Direct	Sensor	Offset	Op.Data1	Op.Data2	Op.Data3	Alarm1	Alarm2
1	date / time	=DATE()		/YYYY HH:								
2	Load	=CH(0)*0.75	KN	0.00	Meas	4GAGE						
3	LVD1-1	=CH(1)*0.01	mm	0.00	Meas	4GAGE						
4	LVD1-2	=CH(2)*0.01	mm	0.00	Meas	4GAGE						
5	LVD1-3	=CH(3)*0.005	mm	0.00	Meas	4GAGE						
6	LVD1-4	=CH(4)*0.005	mm	0.00	Meas	4GAGE						
7	LVD1-5	=CH(5)*0.005	mm	0.00	Meas	4GAGE						
8	LVD1-6	=CH(6)*0.005	mm	0.00	Meas	4GAGE						
9	SFA-1	=CH(7)*2/2.12	μ	0	Meas	AGE 3W 1						
10	SFA-2	=CH(8)*2/2.12	μ	0	Meas	AGE 3W 1						
11	SFA-3	=CH(9)*2/2.12	μ	0	Meas	AGE 3W 1						
12	SFA-4	=CH(10)*2/2.12	μ	0	Meas	AGE 3W 1						
13	SFB-1	=CH(11)*2/2.12	μ	0	Meas	AGE 3W 1						
14	SFB-2	=CH(12)*2/2.12	μ	0	Meas	AGE 3W 1						
15	SFB-3	=CH(13)*2/2.12	μ	0	Meas	AGE 3W 1						
16	SFB-4	=CH(14)*2/2.12	μ	0	Meas	AGE 3W 1						
17												

Figure 10. Format for filling in instrument data

3. Result and Discussion

3.1. Deformation and Cracks

3.1.1. Deformation

The column legs showed swaying characteristics under cyclic lateral loads due to the use of free support placement in wooden structures. The main cause of lateral displacement in each test cycle was attributed to sway of the column, while beam and post connections moved translationally. The typical deformation of tested wooden stilt house structure is shown in Figure 11. Meanwhile, Figure 12 showed a 50 mm slippage between the column foot and the concrete floor during the test.



Figure 11. Deformation of the structure of wooden stilt houses



Figure 12. Translation of columns during testing, (a) before testing, (b) after testing

During the testing procedure, wooden structures showed capacity of returning to starting position without the assistance of external forces. This phenomenon showed the exceptional deformation recovery ability of wooden structures, as observed from different lateral loads in this study. With post-reinforcement, the bending moments at mortise-tenon joints and rocking columns provided the majority of the restoring force for wooden structures.

3.1.2. Cracks in Wooden Components

All structural elements were undamaged and the majority of wooden structures maintained their elasticity. Figure 13 shows plastic deformation and damage in the form of tiny cracks, which are particularly observed in the beam-column, column, and *suddug* connection components. A maximum strain of 331.79 (ϵ_{max}) and a minimum strain of 98 (ϵ_{min}) was also observed, indicating the significance of the connection in lowering seismic energy.

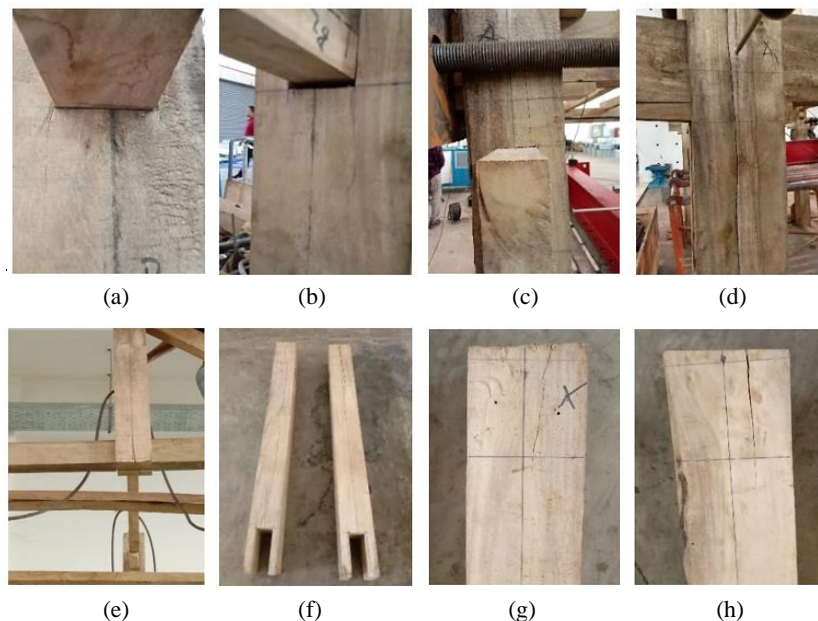


Figure 13. Cracks in structural components, (a-b) Connections between beams and columns, (c-d) Columns, and (e-h) *Suddug*

3.2. Hysterical Behavior

Hysteretic curve is the result of testing structures against cyclic lateral loads occurring frequently. Figure 14 shows hysteretic loop graph, which results in a load capacity (P_{peak}) of 6.06 kN for the compression cycle (+) and 3.3 kN for the tension cycle (-). Specifically, cycle 13 has a maximum average load of 4.70 kN, a maximum displacement of 67.38 mm, and 72.98 for the (+) cycle, and (-) cycle, respectively. Hysteresis graphs from cycles 11, 12, and 13 have the same curve shape, as shown in Figures 15 to 17. After 13 cycles of displacement control, the cyclic testing results for the specimens were approximately in line with the original plan on average for each cycle. The peak strength capacity, stiffness reduction, ductility, and energy dissipation are among the structural performance parameters caused by cyclic lateral loads, as shown in the curve in Figure 14.

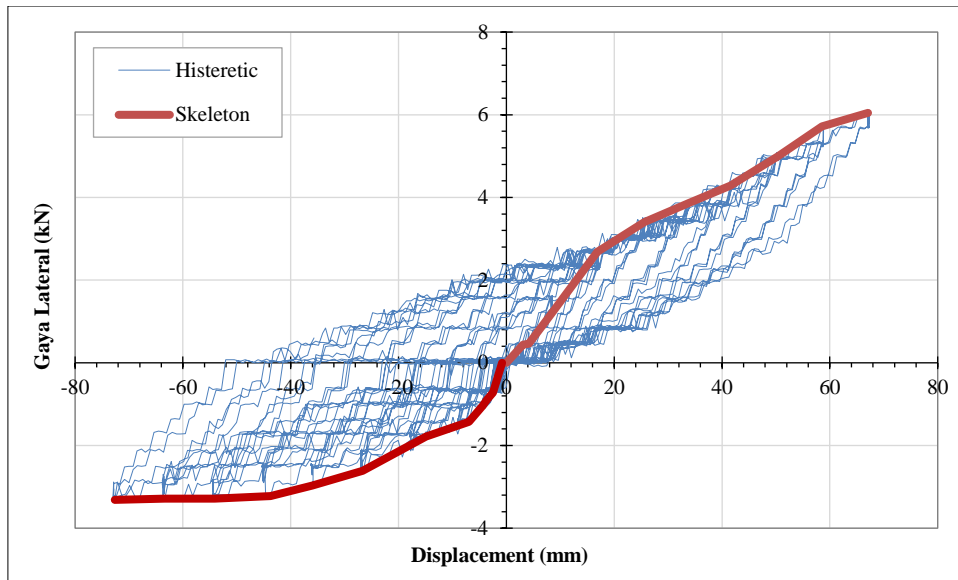


Figure 14. Loop and skeleton hysteresis curves

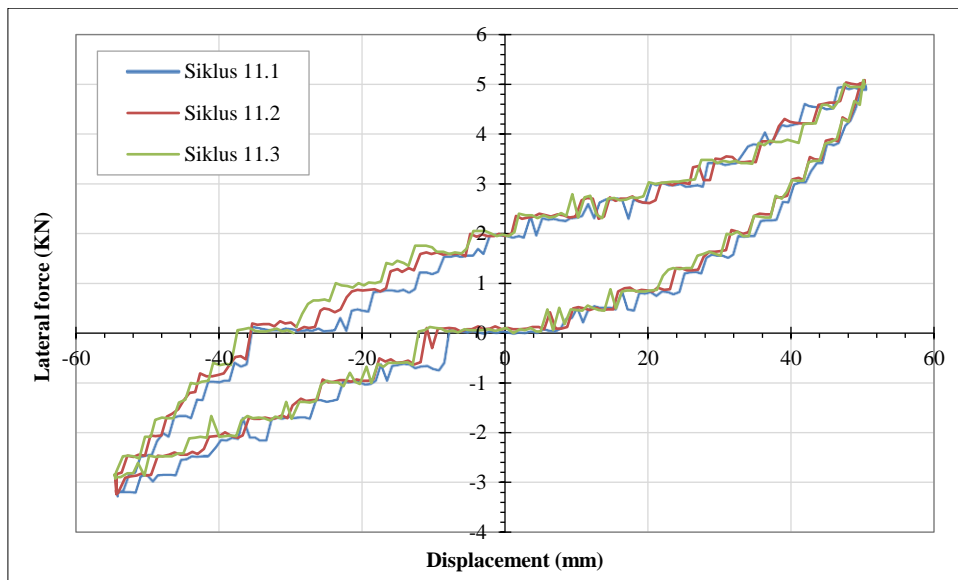


Figure 15. Cycle 11 loop hysteresis curve

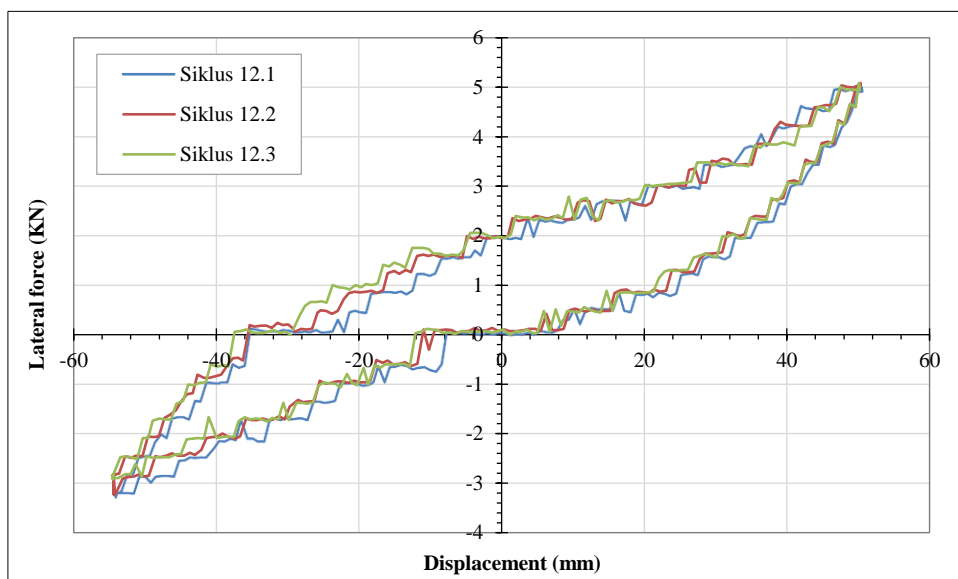


Figure 16. Cycle 12 loop hysteresis curve

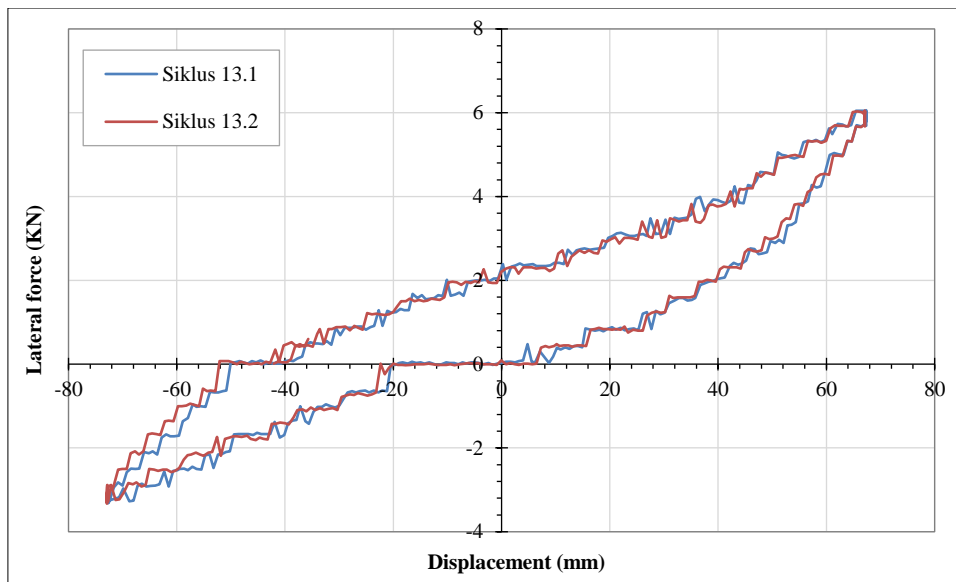


Figure 17. Cycle 13 loop hysteresis curve

A definite pinch is observed in the curve when the lateral displacement (Δ) is at a deviation ratio of 1.25% - 40%, or $-20 \text{ mm} \leq \Delta \leq 20 \text{ mm}$. During this phase, wooden structure is in the elastic stage, with the friction movement between the mortises and tenons serve as the primary source of energy dissipation, resulting in minimal energy loss. As the lateral displacement (Δ) exceeds 20 mm, the curve tends to take on a similar shape, showing the influence of melting on wooden structures. Except for friction movements, the majority of the plastic deformation in the yield stage occurs in wooden beam-column joints and pin components, increasing energy dissipation of the structure. This leads to a more complete hysteresis loop, with curves overlapping for every cycle, specifically in the three-loop cycle tests. The main reason for this resemblance is the rocking motion, effectively preventing damage to the rigidity and bearing capacity of wooden structures. Although at drift ratio of approximately 160%, wooden structures encounter more load paths, there is no discernible drop in lateral load. Specifically, after cycle 13, the test showed that the stability and integrity wooden frame structure remained intact.

3.3. Vertical Movement during Lateral Loads

According to tests conducted, wooden structures above the column moved very stiffly, shifting both laterally and vertically due to swaying under lateral loads. Figure 18 shows the history of vertical displacement in the beam due to the movement of the structure vertically. Despite appearing in translation, these movements suggested that the component above the column was tilting. As the cyclic amplitude increased, both the positive and negative vertical displacements showed a consistent rise, which was significant at cycle 13. Based on the results, the minimum negative vertical displacement was measured at 1.86 mm, while the maximum positive vertical displacement reached 4.28 mm.

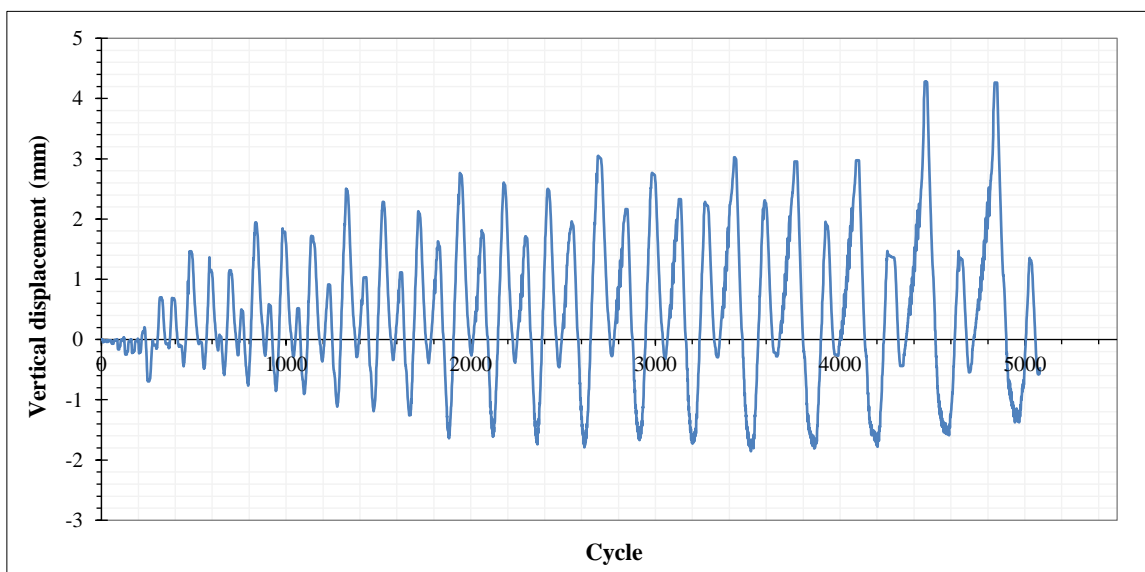


Figure 18. Vertical displacement history

The relationship between the test cyclic amplitude and the vertical displacement obtained is shown in Figure 19, indicating the increasing trend of wooden structures in all directions. The vertical displacement is negligible and can be disregarded when the cyclic amplitude is small, as shown in the positive direction. These results showed that the load of the roof structure has no effect on the structural qualities or rocking.

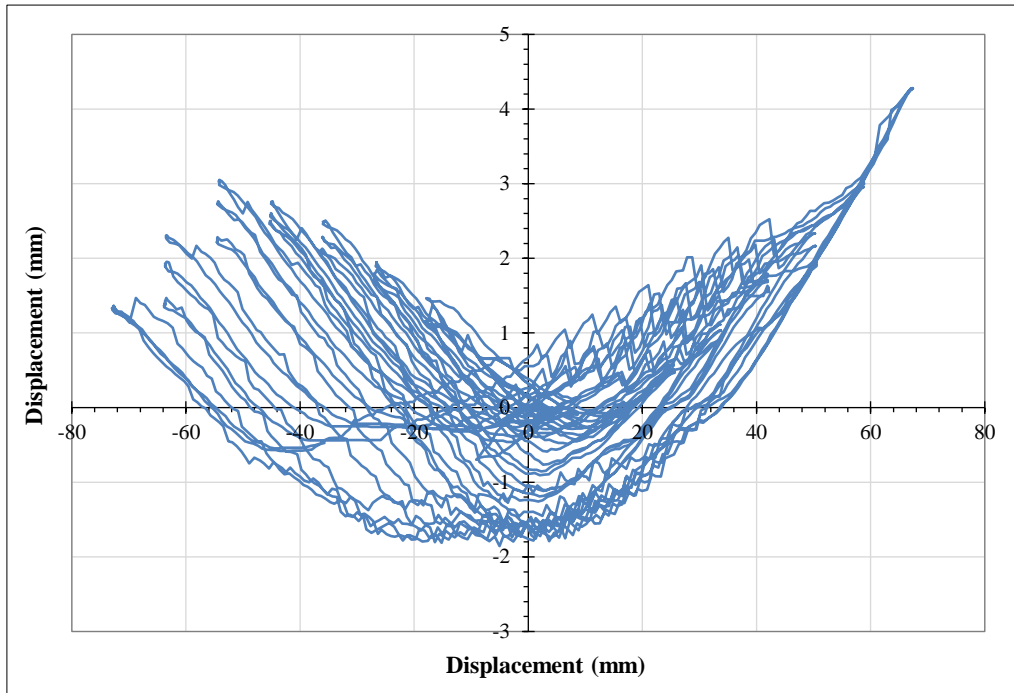


Figure 19. Relationship between vertical displacement and cyclic amplitude

3.4. Yield Displacement and Yield Force

The yield force and yield displacement of specimens K1 (left front column), K2 (right front column), K3 (left rear column), and K4 (right rear column) are obtained from the ultimate force and displacement relationship diagram in Figure 20. The methods used for the analysis are shown in Table 2, including the Karabely and Cettotti (K and C) method, the European Committee for Standardization (CEN), the Commonwealth Scientific and Industrial Research Organization (CSIRO), and the Equivalent Energy Elastic-Plastic Curve (EEEP).

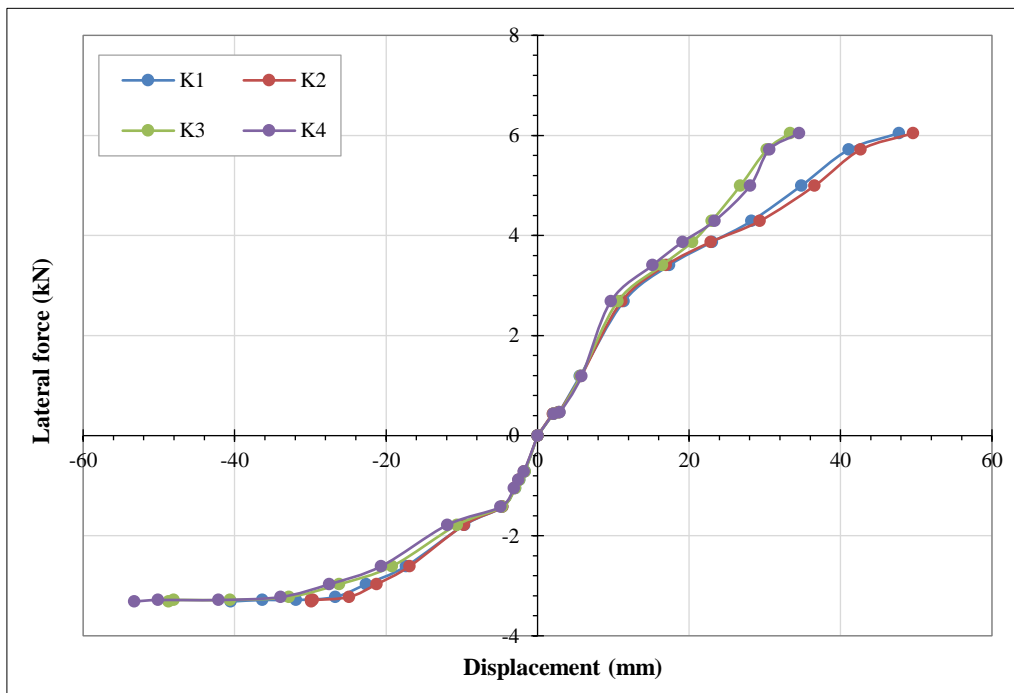


Figure 20. Force and ultimate displacement relationship

Table 2. Values of Yield Force and Yield Displacement

Examine Items	K&C Method		CEN Method		CSIRO Method		EEEP Method	
	P_y (kN)	Δ_y (mm)	P_y (kN)	Δ_y (mm)	P_y (kN)	Δ_y (mm)	P_y (kN)	Δ_y (mm)
K1+	3.023	14.03	3.15	13.03	2.95	13.31	4.84	21.50
K1-	-1.66	-7.95	-1.4	-4.55	-1.44	-4.81	-2.65	-9.45
K2+	3.023	13.50	3.30	13.75	2.93	13.06	4.84	20.75
K2-	-1.66	-8.02	-1.38	-4.35	-1.45	-5.06	-2.65	-8.67
K3+	3.023	13.03	2.95	11.95	2.92	12.31	4.84	19.50
K3-	-1.66	-8.35	-1.38	-4.57	-1.46	-4.94	-2.65	-8.35
K4+	3.023	12.03	3.25	11.75	2.95	11.69	4.84	18.30
K4-	-1.66	-9.36	-1.35	-4.15	-1.44	-4.98	-2.65	-9.46

3.5. Ductility of Structural Components

The mass, stiffness, and capacity of structures to absorb seismic energy influence the reaction earthquake. Specifically, rigid structures tend to attract large internal forces, thereby reducing the effects of earthquakes. The ability of structures or structural elements to pass through inelastic deformation repeatedly while retaining the majority of their initial strength when supporting loads is known as ductility.

Table 3. Ductility of Structural Components

Examine Items	Maximum displacement (mm)	K&C Method		CEN Method		CSIRO Method	
		Yield displacement (mm)	Ductility (mm)	Yield displacement (mm)	Ductility (mm)	Yield displacement (mm)	Ductility (mm)
K1+	47.73	14.03	3.40	13.03	3.66	13.31	3.59
K1-	-40.51	-7.95	5.10	4.55	8.90	4.81	8.42
K2+	49.6	13.5	3.67	13.75	3.61	13.06	3.80
K2-	-29.89	-8.02	3.73	4.35	6.87	5.06	5.90
K3+	33.34	13.03	2.56	11.95	2.79	12.31	2.71
K3-	-48.71	-8.35	5.83	4.57	10.66	4.94	9.87
K4+	34.56	12.03	2.87	11.75	2.94	11.69	2.96
K4-	-53.26	-9.36	5.69	4.15	12.83	4.98	10.71

Ductility of Structural Components (Advanced)

Examine Items	Maximum displacement (mm)	EEEP Method			Average	
		Yield displacement (mm)	Ductility (mm)	Yield displacement (mm)	Ductility (mm)	
K1+	47.73	21.5	2.22	15.47	3.09	
K1-	-40.51	-9.45	4.29	-6.69	6.05	
K2+	49.6	20.75	2.39	15.27	3.25	
K2-	-29.89	-8.67	3.45	-6.53	4.58	
K3+	33.34	19.5	1.71	14.20	2.35	
K3-	-48.71	-8.35	5.83	-6.55	7.43	
K4+	34.56	18.3	1.89	13.44	2.57	
K4-	-53.26	-9.46	5.63	-6.99	7.62	

The displacement ductility, defined as the ratio of ultimate displacement (Δ_u) to initial yield strength (Δ_y) was used to analyze ductility value of each specimen in this study, as shown in Table 3, including Figures 21 and 22. The results showed that the right front column (K2+) had the maximum ductility value under compressive load, with a value of 3.25. Meanwhile, the rear right column (K4-) had the maximum ductility value under tensile load, 7.62. Table 4 classifies each test object's column ductility according to the average value of individual conditions.

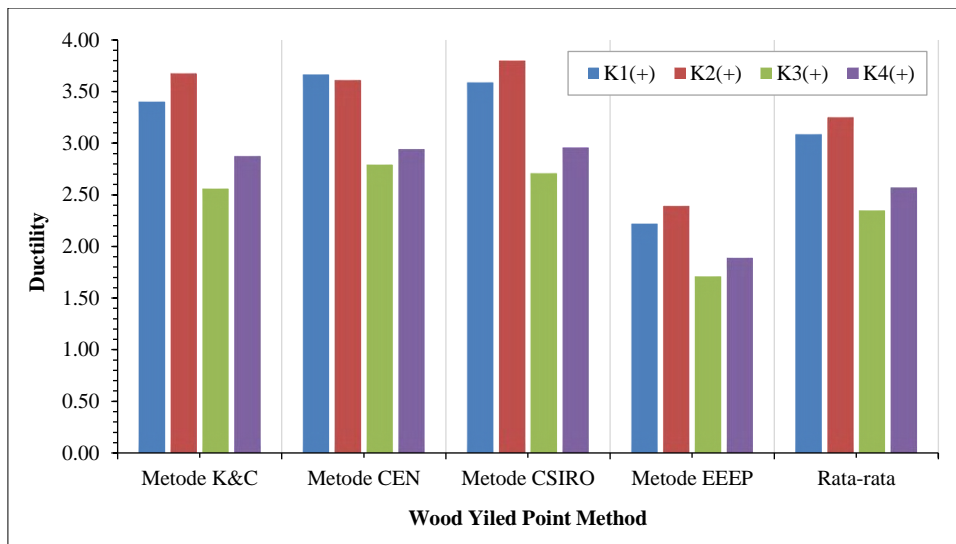


Figure 21. Column structural components' ductility (+)

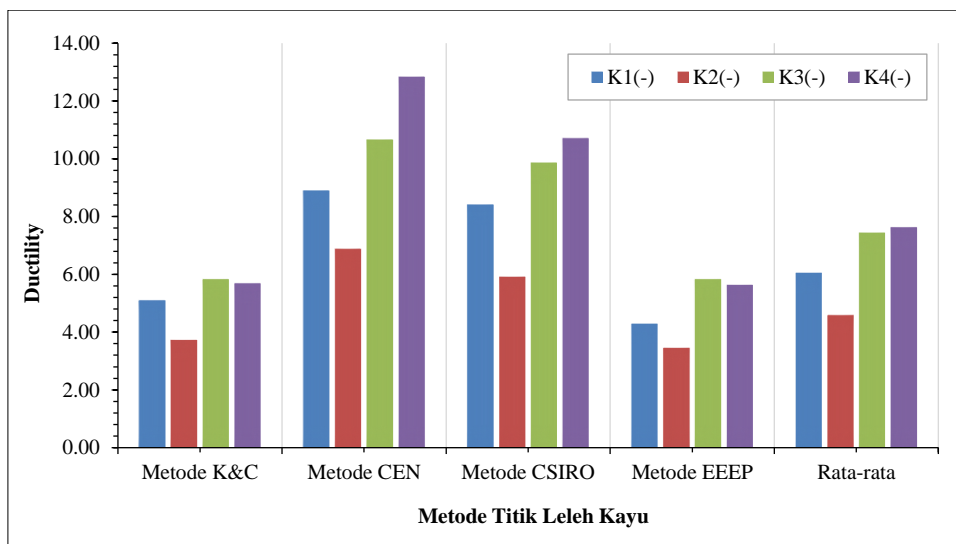


Figure 22. Column structural components ductility (-)

According to the ASCE 41-17 classification, components with a ductility value of less than two fall into the low category. Meanwhile, values between two and four are classified as medium, and values greater than four are considered high [45]. The average ductility of wooden structural column specimens obtained in this study was included in the high ductility category based on the classification.

Table 4. Test specimens' ductility classification in accordance with ASCE 41-17

Examine Items	K&C Method	CEN Method	CSIRO Method	EEEP Method	Average	Classification
	Ductility	Ductility	Ductility	Ductility	Ductility	
	(mm)	(mm)	(mm)	(mm)	(mm)	
K1+	3.40	3.66	3.59	2.22	3.09	Medium ductility
K1-	5.10	8.90	8.42	4.287	6.05	High ductility
K2+	3.67	3.61	3.80	2.39	3.25	Medium ductility
K2-	3.73	6.87	5.90	3.45	4.58	High ductility
K3+	2.56	2.79	2.71	1.71	2.35	Medium ductility
K3-	5.83	10.66	9.87	5.83	7.43	High ductility
K4+	2.87	2.94	2.96	1.89	2.57	Medium ductility
K4-	5.69	12.83	10.71	5.63	7.62	High ductility

A more comprehensive understanding of the seismic behavior of Bugis-Makassar stilt timber structures can be obtained by comparing the results of full-scale experimental tests with analytical or computational models. Because full-scale experimental tests involve actual physical structures, they typically offer a more direct picture of seismic behavior. Conversely, analytical or computational models offer more control over specific variables and enable virtual testing under a variety of circumstances. Pre-test analysis was done with the ETABS application, just like in Figure 23. The base force, which is significantly higher than the experimental test results at 89.15 KN, is demonstrated by the results.

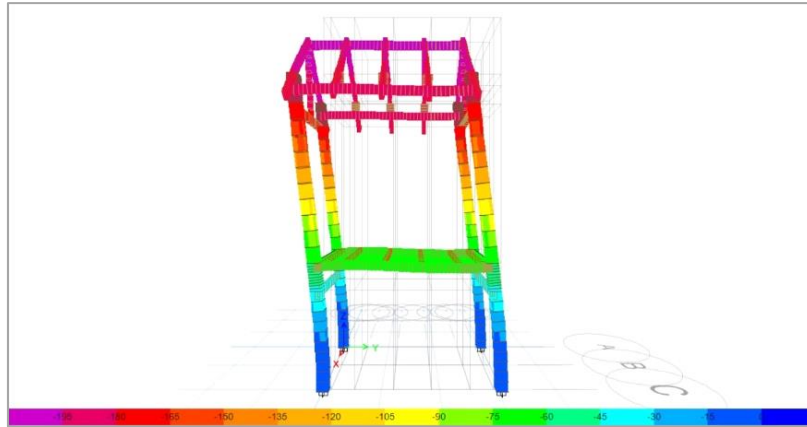


Figure 23. Pretest analysis using the ETABS numerical application

3.6. Analysis of Seismic Mechanisms Based on Energy

3.6.1. Energy Equation

The energy relationship in a structure can be expressed as follows after an earthquake:

$$E_I = E_{\xi} + E_K + E_H + E_E \tag{1}$$

where E_I is the input energy, E_{ξ} is the damping energy, E_K is the kinetic energy, E_H is the hysteretic energy, and E_E is the elastic strain energy (ESE), according to Uang and Bertero (1988, 1990) [46, 47]. Since the velocity in this equation is almost zero, or $v = 0.15$ mm/s, E_{ξ} and E_K , are disregarded during the cyclic tests carried out. Furthermore, the results show that under lateral loads, wooden structures undergo uplift, where a portion of energy applied to the structure during loading is transformed into gravitational potential energy (GPE) and stored. Consequently, the energy equation for a wooden structure in cyclic testing can be expressed as follows:

$$E_I = E_H + E_G + E_E \tag{2}$$

where E_H is the hysteretic energy dissipated by wooden structure due to friction and plastic deformation of wooden components. E_G and E_E are the converted GPE and elastic stress energy (ESE), respectively, and E_I is the total energy input to wooden structures by lateral load. Specifically, the recoverable energy stored in the structure is represented by E_G and E_E , which are integrally denoted as E_R . Figure 24 shows the graphical representation of displacement and load.

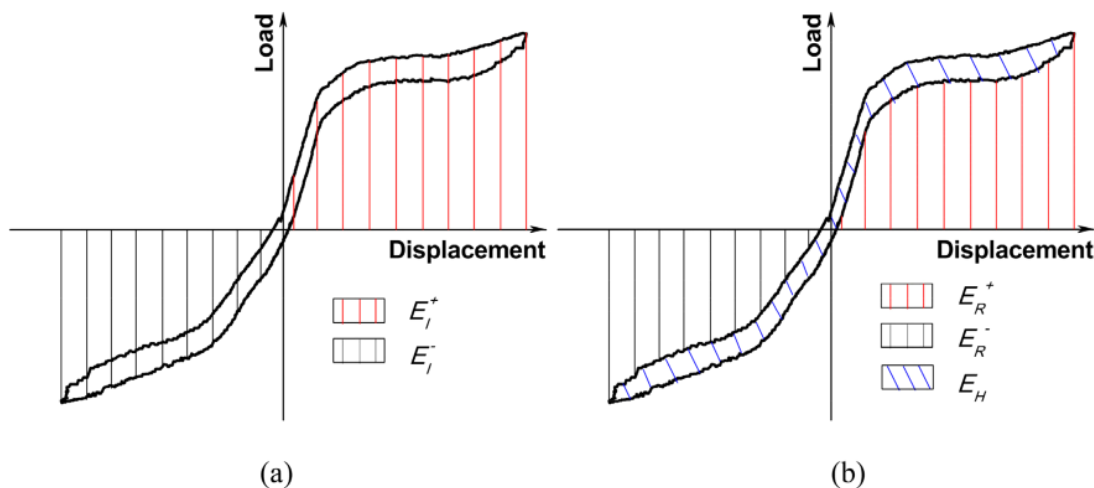


Figure 24. (a) Illustration of E_I , (b) E_R and E_H

3.6.2. Total Energy Input E_I

The work performed by lateral loads can be used to express the total energy input of a wooden structure. The expression is computed as the area of the shaded region in Figure 24-a for every cycle, an example of the energy input during the previous three cycles. In all tests shown in Figure 25, the input energy rises linearly with increasing cyclic amplitude.

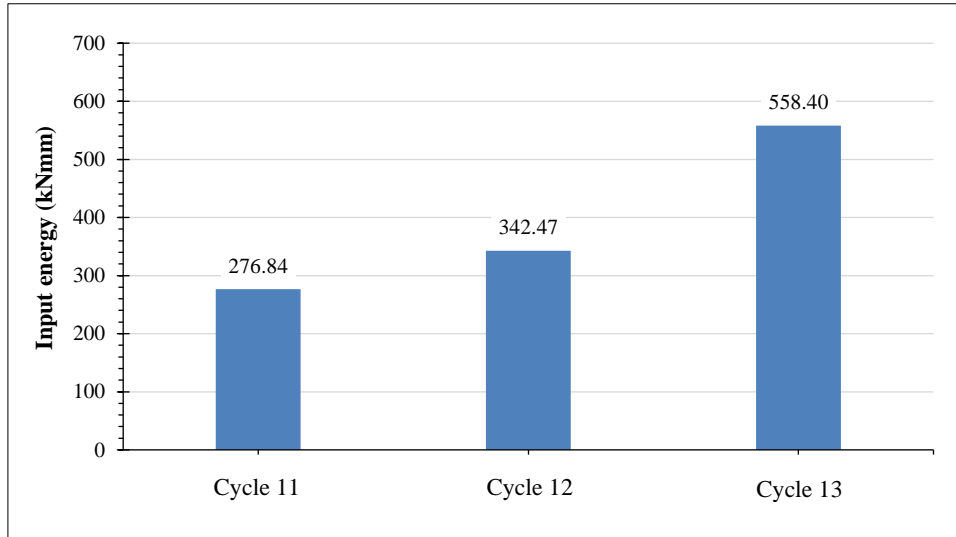


Figure 25. Input Energy (E_I)

E_I was 276.84 kNmm in Cycle 11, 342.47 kNmm in Cycle 12, and 558.404 kNmm in Cycle 13, according to the computation results.

3.6.3. Hysterical Energy (E_H)

The area of the shaded area of hysteresis curve, as shown in Figures 26 to 28, is used to calculate hysteretic energy.

E_H in Cycles 11, 12, and 13 was 164.75 kNmm, 201.25 kNmm, and 197.45 kNmm, respectively, according to the computation results that matched the hysteresis energy graph. This showed that as the cyclic amplitude increased during the test, along with energy dissipated by wooden structure. The increase can be attributed to the increase in lateral displacement, leading to plastic deformation of orthogonal contact surfaces and relative slip between components. Figure 29 shows hysteretic energy to input energy ratio for the last three cycles.

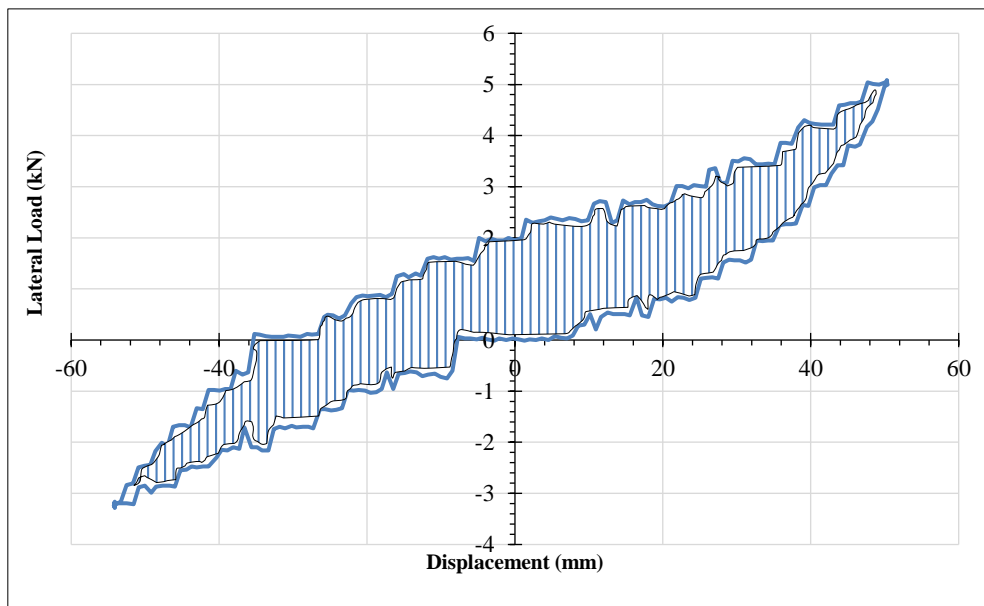


Figure 26. Hysteresis energy of wooden house structures (Cycle 11)

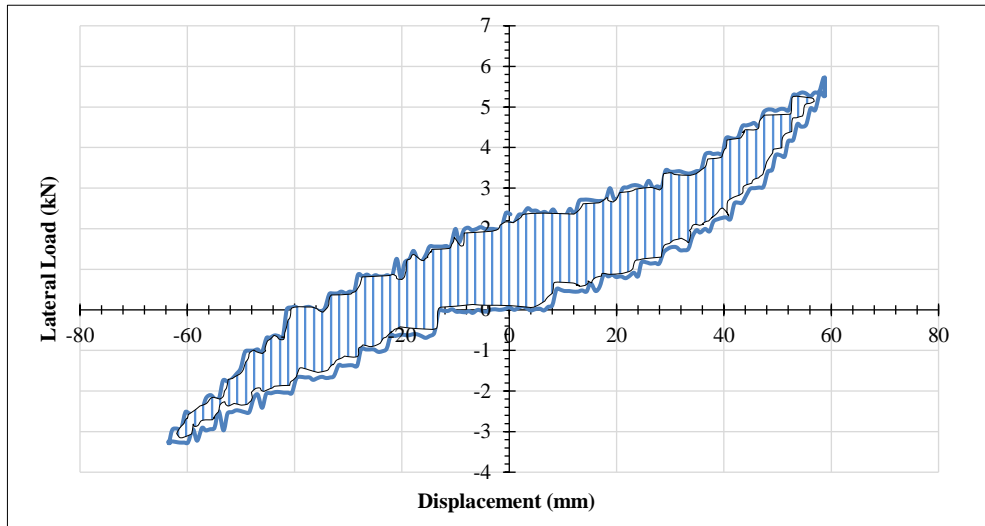


Figure 27. Hysteresis energy of wooden house structures (Cycle 12)

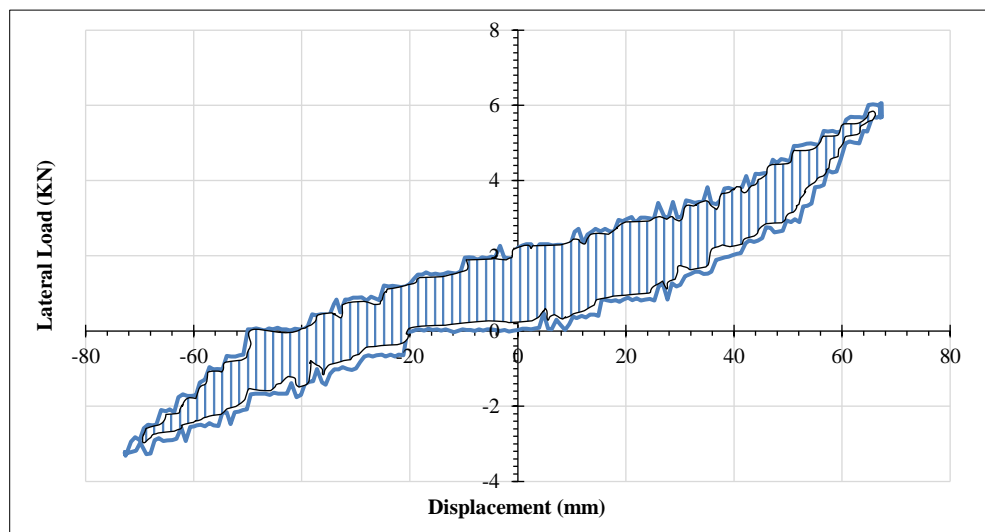


Figure 28. Hysteresis energy of wooden house structures (Cycle 13)

The conversion of the total input to hysteretic energy showed a balanced contribution from elastic strain and gravitational potential energy. All ratios are below 70%, with a mean of 51%, consistently declining over the last three cycles as amplitude rises, with cycle 13 experiencing a sharp decline reaching 34%. These results suggested that in cycles where the cyclic amplitude is greater than the elastic limit, wooden structure dissipates the input energy at an approximately constant ratio.

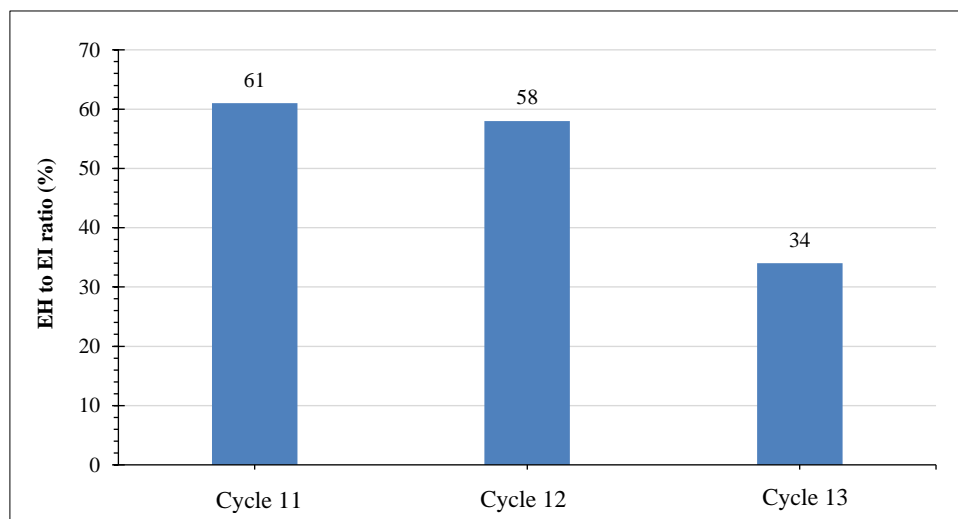


Figure 29. Ratio of Hysteresis Energy (E_H) to Input Energy (E_I)

There are numerous important practical implications of the energy conversion mechanism used to increase the earthquake resistance of Bugis-Makassar wooden stilt house structures. Wooden stilt house constructions can be engineered to more efficiently absorb and redirect seismic energy through the use of energy conversion mechanisms. In the event of an earthquake, this can lessen the load on the main structure and preserve the building's structural integrity. During earthquakes, energy conversion devices can lessen the structural damage done to wooden stilt homes. It is possible to reduce damage to the main structure and other significant components by building a system that can absorb vibration energy. Residents of wooden stilt houses will feel safer during an earthquake because of their increased resistance to seismic activity. The chance of harm or even death from a building collapsing can be decreased if a structure is able to withstand and not collapse. Energy conversion mechanisms have the potential to lower repair and maintenance costs following an earthquake by mitigating structural damage. This can be a significant factor, particularly for local communities that reside in seismically vulnerable areas like Bugis-Makassar, where seismic activity poses a serious risk. Enhancing the resilience of wooden stilt houses to earthquakes can also lead to more environmental sustainability. Because earthquake-resistant homes typically need fewer repairs and upkeep over time, the environmental impact of building construction and repair can be minimized. Energy conversion mechanisms can significantly improve resilience, safety, and sustainability when incorporated into the design and construction of wooden stilt houses in earthquake-prone areas like Bugis-Makassar.

3.6.4. Energy conversion Elastic Tension Energy and Gravitational Potential Energy (E_R)

The energy that can be recovered and stored within a structure is known as E_R , or the conversion energy between gravitational potential energy (GPE) and elastic stress energy (ESE). The expression of the conversion energy is computed as the area of shaded region in Figure 24-b for every cycle. In this study, E_R was 107.10 kNmm, 141.22 kNmm, and 360.95 kNmm, in Cycles 11, 12, and 13 respectively, according to the computation results.

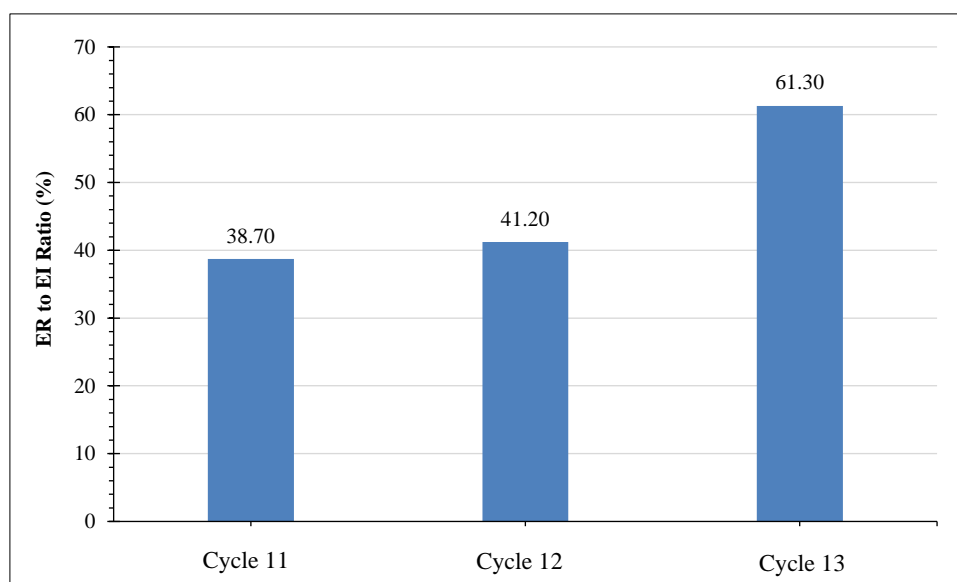


Figure 30. Ratio of GPE and ESE (E_R) to Energy Input (E_I)

The results show that throughout the test, the cyclic amplitude of the energy stored in wooden structure increased. Figure 30 shows the ratios of E_R to E_I for the previous three cycles, which are below 70%, with an average of 47%. Consequently, when earthquake occurs, energy conversion mechanism to GPE and ESE is less than hysteresis energy, showing a lower possibility of cracking in wooden structural components.

Traditional wooden houses can perform better seismically in a number of ways thanks to research on the significance of mechanical energy conversion in enhancing the earthquake resistance of wooden stilt house structures. The development of technologies that can be used in the construction of traditional wooden houses can be facilitated by research on efficient energy conversion mechanisms. Traditional wooden building designs can incorporate technology made expressly to absorb and redirect seismic energy. The structural design of traditional wooden houses could be influenced by discoveries about energy conversion mechanisms to increase their earthquake resistance. To improve seismic performance, this can entail modifying the overall structural configuration or adding structural elements that can absorb earthquake energy. Although wood is the primary material used in traditional wooden houses, contemporary materials with good energy conversion qualities can also be used. For instance, the seismic performance of wooden homes can be enhanced by the installation of contemporary vibration dampers or bearings composed of composite or elastomeric materials. It's critical to inform traditional log home builders about the value of applying new technologies in design and construction as well as the significance of seismic performance.

Traditional wooden houses can be made more earthquake-resistant by receiving training on how to incorporate energy conversion principles into building practices. The seismic performance of traditional wooden house structures can be assessed through dynamic testing or simulated earthquake test methods. The public can feel more confident about the safety and dependability of traditional wooden houses when they are certified as earthquake-resistant. Through the application of energy conversion mechanism research findings in traditional wooden house construction and design, we can enhance the seismic performance of these structures and raise the safety of residents in areas vulnerable to earthquakes.

4. Conclusions

In conclusion, this study showed the significance of the energy conversion mechanism in enhancing the seismic resilience of wooden structures. Based on the analysis conducted, the following information was obtained regarding the seismic behavior of Bugis-Makassar stilt house structures.

- Lateral loads caused sway in wooden structures but showed resistance to damage due to the weak energy dissipation capacity caused by their rocking behavior. With the restoring force supplied by the column sway and the bending moment of the post-reinforced mortise-tenon connection, the wooden structure showed excellent deformation recovery.
- Lateral loads led to lifting in wooden structures, causing an increase in displacement along with column inclination. Although small vertical displacement was obtained in the wooden structures, consideration must be taken when examining the seismic mechanism and the possibility of roof structure lifting.
- According to the results, the Bugis-Makassar stilt house structures showed good structural behavior or characteristics such as strength, ductility, stiffness, and energy dissipation in response to seismic loads.
- The input energy to wooden structures was divided into three components, namely: (1) hysteretic energy dissipated by the structure through plastic deformation and friction; (2) gravitational potential energy (GPE) converted through structural enhancement; and (3) elastic stress energy (ESE) converted by the elastic deformation of wood components. The hysteretic energy and ESE for the majority of the input energy were converted at small cyclic amplitudes, which were mostly transformed into GPE at large cyclic amplitudes.
- The conversion ratio of hysteretic energy to input energy was 51%, while GPE and ESE (E_R) to input energy was 47% for large cyclic amplitudes. This approximately balanced ratio between E_R and E_H to E_I , enabling the repetitive storage and release of seismic energy to reduce damage to structural elements.
- Research on the seismic behavior of traditional Bugis-Makassar wooden stilt houses may move forward with the creation of models and repair strategies. Next, a more precise model to forecast the seismic behavior of wooden stilt houses needs to be developed based on the findings of data analysis and the identification of determining factors. These models could be more complex experimental models, computer simulations, or mathematical models. The next step was to develop suitable repair or repair solutions after weaknesses in the seismic performance of wooden stilt houses were discovered in the form of tiny cracks, particularly in beam-column connections with post reinforcement. may involve the creation of new technology, adjustments to the structural design, or adjustments to the methods used in construction. Future research on the Bugis-Makassar stilt houses and seismic resistance can concentrate on a few specific areas, such as a detailed analysis of the impact of conventional building materials and methods on the seismic resistance of the stilt houses. This includes a thorough examination of the conventional materials' strength, elasticity, and dynamic behaviour.

5. Declarations

5.1. Author Contributions

Conceptualization, A.A. and H.P.; methodology, A.A.; software, A.A.; validation, H.P., R.I., and A.A.A.; formal analysis, A.A.; investigation, A.A.; resources, A.A.; data curation, A.A.; writing—original draft preparation, A.A.; writing—review and editing, A.A.; visualization, A.A.; supervision, H.P., R.I., and A.A.A.; project administration, A.A.; funding acquisition, A.A. All authors have read and agreed to the published version of the manuscript.

5.2. Data Availability Statement

The data presented in this study are available on request from the corresponding author.

5.3. Funding

The authors received financial support from the Center for Education Financial Service (PUSLAPDIK) and Indonesia Endowment Funds for Education (LPDP), Ministry of Finance of the Republic of Indonesia, for the publication of this study.

5.4. Acknowledgements

The first author of this study is grateful to the Center for Education Financial Service (PUSLAPDIK) and LPDP (Indonesia Endowment Fund for Education), Ministry of Finance, Republic Indonesia for providing financial support for doctoral study at Hasanuddin University, Indonesia.

5.5. Conflicts of Interest

The authors declare no conflict of interest.

6. References

- [1] Kaharuddin, M. S., Hutagalung, R., & Nurhamdan, N. (2011). Tectonic developments and their implications for the potential for earthquakes and tsunamis in the Sulawesi Island area. The 36th HAGI and 40th IAGI Annual Convention and Exhibition, 26-29 September, 2011, Makassar, Indonesia. (In Indonesian).
- [2] Indonesia-Investment. (2018). Natural Disasters in Indonesia. Indonesia-Investment, Bantul, Indonesia. Available online: <https://www.indonesia-investments.com/business/risks/natural-disasters/item243> (accessed on March 2024).
- [3] BIG. (2023). Indonesian Ballad InaTEWS and Disaster. Geospatial Information Agency, Jakarta, Indonesia. Available online: <https://big.go.id/en/content/article/indonesian-ballad-inatews-and-disaster> (accessed on January 2024).
- [4] Reuters Graphics. (2018). Catastrophe in Sulawesi. Available online: <https://fingfx.thomsonreuters.com/gfx/rngs/INDONESIA-QUAKE/010080KV15C/index.html> (accessed on March 2024).
- [5] Sudarman, S., & Attar, M. (2020). Study of Vernacular House Endurance in South Sulawesi To Earthquake as a Result of Quality Change in Structure Material. *Vitruvian Journal of Building Architecture and Environment*, 10(1), 61. doi:10.22441/vitruvian.2020.v10i1.008.
- [6] PUPR. (2021). Review and Analysis of Indonesia Traditional House. Research Institute for Human Settlements (PUPR), Jakarta, Indonesia.
- [7] Idham, N. C. (2021). Directing Housing Developments for Achieving Earthquake Disasters Safety in Indonesia. *IOP Conference Series: Earth and Environmental Science*, 933(1), 012035. doi:10.1088/1755-1315/933/1/012035.
- [8] Prihatini, Z. & Dewi, B.K. (2021). Why was the NTT earthquake felt in Makassar? This is an expert explanation. Jakarta, Indonesia. Available online: https://www.kompas.com/sains/read/2021/12/15/070500523/mengapa-gempa-ntt-terasa-hingga-makassar-ini-penjelasan-pakar?page=all#google_vignette (accessed on March 2024).
- [9] Parung, H. (2012). Seismic Design of Building. UNM Publisher Makassar, Sulawesi Selatan, Indonesia.
- [10] Sari, D. P., Sudirman, M., & Asmuliany, A. (2024). The Design of Earthquake Evacuation Spaces Based on Local Wisdom: A Case Study of Traditional Houses in South Sulawesi. *Designs*, 8(2), 30. doi:10.3390/designs8020030.
- [11] Barreca, F., Arcuri, N., Cardinali, G. D., Fazio, S. Di, Rollo, A., & Tirella, V. (2022). A Highly Sustainable Timber-Cork Modular System for Lightweight Temporary Housing. *Civil Engineering Journal (Iran)*, 8(10), 2336–2352. doi:10.28991/CEJ-2022-08-10-020.
- [12] Doğan, M. (2010). Seismic analysis of traditional buildings: Bagdadi and Himis. *Anadolu University Journal of Science and Technology A-Applied Sciences and Engineering*, 11(1), 35-45.
- [13] Doğan, A., Tuluk, Ö. I., Livaoglu, R., & Acar, R. (2006). Traditional wooden buildings and their damages during earthquakes in Turkey. *Engineering Failure Analysis*, 13(6), 981–996. doi:10.1016/j.engfailanal.2005.04.011.
- [14] Erarslan, A. (2019). Timber construction systems in anatolian vernacular architecture. *Bulletin of the Transilvania University of Brasov, Series II: Forestry, Wood Industry, Agricultural Food Engineering*, 12(2), 37–52. doi:10.31926/but.fwiawe.2019.12.61.2.3.
- [15] Aktaş, Y. D. (2017). Seismic resistance of traditional timber-frame himiş structures in Turkey: a brief overview. *International Wood Products Journal*, 8, 21–28. doi:10.1080/20426445.2016.1273683.
- [16] Güçhan, N. Ş. (2018). History and Characteristics of Construction Techniques Used in Traditional Timber Ottoman Houses. *International Journal of Architectural Heritage*, 12(1), 1–20. doi:10.1080/15583058.2017.1336811.
- [17] Bağbancı, M. B., & Bağbancı, Ö. K. (2018). The Dynamic Properties of Historic Timber-Framed Masonry Structures in Bursa, Turkey. *Shock and Vibration*, 2018. doi:10.1155/2018/3257434.
- [18] Chand, B., Kaushik, H. B., & Das, S. (2020). Material Characterization of Traditional Assam-Type Wooden Houses in Northeastern India. *Journal of Materials in Civil Engineering*, 32(12), 10 1061 1943–5533 0003492. doi:10.1061/(asce)mt.1943-5533.0003492.
- [19] Chand, B., Kaushik, H. B., & Das, S. (2020). Lateral load behavior of connections in Assam-type wooden houses in the Himalayan region of India. *Construction and Building Materials*, 261. doi:10.1016/j.conbuildmat.2020.119904.

- [20] Paudel, S., Shima, N., & Fujii, T. (2018). Development of earthquake resilient housing in Nepal by development of earthquake introducing Japanese. *AIJ Journal of Technology and Design*, 24(57), 751–755. doi:10.3130/aijt.24.751.
- [21] Buchanan, A., & Moroder, D. (2017). Log house performance in the 2016 Kaikoura earthquake. *Bulletin of the New Zealand Society for Earthquake Engineering*, 50(2), 225–236. doi:10.5459/bnzsee.50.2.225-236.
- [22] HORIE, T., & KANEKO, S. (2017). Arrangement and Terminology of the Main Structural Members of the Understructure in Japanese and British Vernacular Houses. *Journal of Architecture and Planning (Transactions of AIJ)*, 82(740), 2553–2563. doi:10.3130/aija.82.2553.
- [23] Kim, Y. M. (2020). Structural analysis and conceptual seismic design of large-span Korean traditional timber structure. *Civil Engineering and Architecture*, 8(2), 154–165. doi:10.13189/cea.2020.080213.
- [24] Vasconcelos, G., Lourenço, P. B., & Poletti, E. (2015). *An Overview on the Seismic Behaviour of Timber Frame Structures. Historical Earthquake-Resistant Timber Frames in the Mediterranean Area*. Springer, Cham, Switzerland. doi:10.1007/978-3-319-16187-7_10.
- [25] Crayssac, E., Song, X., Wu, Y., & Li, K. (2018). Lateral performance of mortise-tenon jointed traditional timber frames with wood panel infill. *Engineering Structures*, 161, 223–230. doi:10.1016/j.engstruct.2018.02.022.
- [26] Dzhurko, D., Haacke, B., Haberbosch, A., Köhne, L., König, N., Lode, F., Marx, A., Mühlnickel, L., Neunzig, N., Niemann, A., Polewka, H., Schmidtke, L., Von der Groeben, P. L. M., Wagemann, K., Thoma, F., Bothe, C., & Churkina, G. (2024). Future buildings as carbon sinks: Comparative analysis of timber-based building typologies regarding their carbon emissions and storage. *Frontiers in Built Environment*, 1330105. doi:10.3389/fbuil.2024.1330105.
- [27] Premrov, M., & Žegarac Leskovar, V. (2023). Innovative Structural Systems for Timber Buildings: A Comprehensive Review of Contemporary Solutions. *Buildings*, 13(7), 13. doi:10.3390/buildings13071820.
- [28] Meng, X., Yang, Q., Wei, J., & Li, T. (2018). Experimental investigation on the lateral structural performance of a traditional Chinese pre-Ming dynasty timber structure based on half-scale pseudo-static tests. *Engineering Structures*, 167, 582–591. doi:10.1016/j.engstruct.2018.04.077.
- [29] Huang, H., Sun, Z., Guo, T., & Li, P. (2017). Experimental study on the seismic performance of traditional Chuan-Dou style wood frames in Southern China. *Structural Engineering International*, 27(2), 246–254. doi:10.2749/101686617X14881932435817.
- [30] Meng, X., Li, T., & Yang, Q. (2019). Experimental study on the seismic mechanism of a full-scale traditional Chinese timber structure. *Engineering Structures*, 180, 484–493. doi:10.1016/j.engstruct.2018.11.055.
- [31] Sha, B., Xie, L., Yong, X., & Li, A. (2021). Hysteretic behavior of an ancient Chinese multi-layer timber substructure: A full-scale experimental test and analytical model. *Journal of Building Engineering*, 43. doi:10.1016/j.job.2021.103163.
- [32] Yu, P., Li, T., & Yang, Q. (2023). Inelastic Behavior of Mortise-Tenon Jointed Traditional Timber Frame with Free-Standing Columns. *International Journal of Architectural Heritage*. doi:10.1080/15583058.2023.2203669.
- [33] Ren, Q., Liang, B., Zhou, Y., Liu, G., Yang, Y., & Lu, L. (2024). Experimental Study on Wooden Pin Reinforcement of the Typical Mortise-Tenon Joints of Ancient Timber Frames. *International Journal of Architectural Heritage*. doi:10.1080/15583058.2024.2320408.
- [34] Li, S., Li, D., Chen, T., Milani, G., Shi, S., & Wang, S. (2023). Seismic performance of timber through-tenon joints with shrinkage flaw in tenon. *Journal of Building Engineering*, 65, 105702. doi:10.1016/j.job.2022.105702.
- [35] Atika, F. A. (2018). Transformation of the Architectural Form of a Bugis Traditional House on Jalan Usman Sadar III/36, Gresik. *Prosiding Seminar Nasional Sains Dan Teknologi Terapan*, September, 2018. (In Indonesian).
- [36] Al-Faaruuq, A. M., & AS, Z. (2020). Local Wisdom of the Bugis Baranti Traditional House in Sidrap Regency. *Timpalaja: Architecture Student Journals*, 2(1), 68–71. doi:10.24252/timpalaja.v2i1a8. (In Indonesian).
- [37] Nawawi, N. (2020). Technology for Building a Bugis House According to Panrita Bola Ugi. *Technoscience: Science and Technology Information Media*, 14(1), 12943. doi:10.24252/teknosains.v14i1.12943. (In Indonesian).
- [38] Puspitasari, S. D., Suprpto Siswosukarto, Harahap, S., & Pinta Astuti. (2022). Analysis of the Behavior and Resistance of Bugis Traditional Houses Against Earthquake Loads. *Jurnal Teknik Sipil*, 16(4), 280–288. doi:10.24002/jts.v16i4.5666.
- [39] Aryadi, A., Kahar, M. A., & Mardiana, R. (2022). Analysis of Response and Performance of Bugis-Makassar Stilt House Structures Using Pushover Analysis. *IOP Conference Series: Earth and Environmental Science*, 1117(1), 012032. doi:10.1088/1755-1315/1117/1/012032.
- [40] Basri, E., Saefudin, Rulliaty, S., & Yuniarti, K. (2009). Drying conditions for 11 potential ramin substitutes. *Journal of Tropical Forest Science*, 328–335.
- [41] Burley, A. L., Enright, N. J., & Mayfield, M. M. (2011). Demographic response and life history of traditional forest resource tree species in a tropical mosaic landscape in Papua New Guinea. *Forest Ecology and Management*, 262(5), 750–758. doi:10.1016/j.foreco.2011.05.008.

- [42] Aryadi, A., Parung, H., Irmawaty, R., & Amiruddin, A. A. (2023). Physical and Mechanical Properties of Bitti Wood in Bugis-Makassar Stilt House Structures. *Prosiding Seminar Nasional Teknik Sipil UMS*, May 2023.
- [43] Armin Aryadi, A. A., Parung, H., Irmawaty, R., & Amiruddin, A. (2023). Structural Design and Construction of Bugis-Makassar Stilt Houses Using BIM (Building Information Modeling) Applications. *Prosiding-Snekti*, 3.
- [44] ISO 16670:2003 (2003). Timber structures - Joints made with mechanical fasteners - Quasi-static reversed-cyclic test method. International Organization for Standardization (ISO), Geneva, Switzerland.
- [45] ASCE/SEI 41-17. (2017). Seismic Evaluation and Retrofit of Existing Buildings. American Society of Civil Engineers (ASCE), Reston, United States. doi:10.1061/9780784414859
- [46] Uang, C. M., & Bertero, V. V. (1988). Implications of recorded earthquake ground motions on seismic design of building structures. Earthquake Engineering Research Center, College of Engineering, University of California, Berkeley, United States.
- [47] Uang, C. M., & Bertero, V. V. (1990). Evaluation of seismic energy in structures. *Earthquake Engineering & Structural Dynamics*, 19(1), 77–90. doi:10.1002/eqe.4290190108.